Inorganic Chemistry

Article

pubs.acs.org/IC

Lead(II) Complex Formation with L-Cysteine in Aqueous Solution

Farideh Jalilehvand,*[,†] Natalie S. Sisombath,[†] Adam C. Schell,[†] and Glenn A. Facey[‡]

[†]Department of Chemistry, University of Calgary, 2500 University Drive NW, Calgary, Alberta T2N 1N4, Canada

[‡]Department of Chemistry, University of Ottawa, 10 Marie Curie Private, Ottawa, Ontario K1N 6N5, Canada

Supporting Information

ABSTRACT: The lead(II) complexes formed with the multidentate chelator L-cysteine (H_2Cys) in an alkaline aqueous solution were studied using ^{207}Pb, ^{13}C, and ^{1}H NMR, Pb L_{III}-edge X-ray absorption, and UV−vis spectroscopic techniques, complemented by electrospray ion mass spectrometry (ESI-MS). The H_2Cys/Pb^{II} mole ratios were varied from 2.1 to 10.0 for two sets of solutions with $C_{Pb^{II}}$ = 0.01 and 0.1 M, respectively, prepared at pH values (9.1−10.4) for which precipitates of lead(II) cysteine dissolved. At low H_2Cys/Pb^{II} mole ratios (2.1−3.0), a mixture of the dithiolate $[Pb(S,N\text{-}Cys)_2]^{2-}$ and $[Pb(S,N,O\text{-}Cys)(S\text{-}HCys)]^{-}$ complexes with average Pb−(N/O) and Pb−S distances of 2.42 ± 0.04 and 2.64 ± 0.04 Å, respectively, was found to dominate. At high concentration of free cysteinate (>0.7 M), a significant amount converts to the trithiolate $[Pb(S,N\text{-}Cys)(S\text{-}HCys)_2]^{2-}$, including a minor amount of a PbS_3-coordinated $[Pb(S\text{-}HCys)_3]^{-}$ complex. The coordination mode was evaluated by fitting linear combinations of EXAFS oscillations to the experimental spectra and by examining the ^{207}Pb NMR signals in the chemical shift range δ_{Pb} = 2006−2507 ppm, which became increasingly deshielded with increasing free cysteinate concentration. One-pulse magic-angle-spinning (MAS) ^{207}Pb NMR spectra of crystalline $Pb(aet)_2$ (Haet = 2-aminoethanethiol or cysteamine) with PbS_2N_2 coordination were measured for comparison (δ_{iso} = 2105 ppm). The UV−vis spectra displayed absorption maxima at 298−300 nm ($S^- \rightarrow Pb^{II}$ charge transfer) for the dithiolate $PbS_2N(N/O)$ species; with increasing ligand excess, a shoulder appeared at ∼330 nm for the trithiolate PbS_3N and PbS_3 (minor) complexes. The results provide spectroscopic fingerprints for structural models for lead(II) coordination modes to proteins and enzymes.

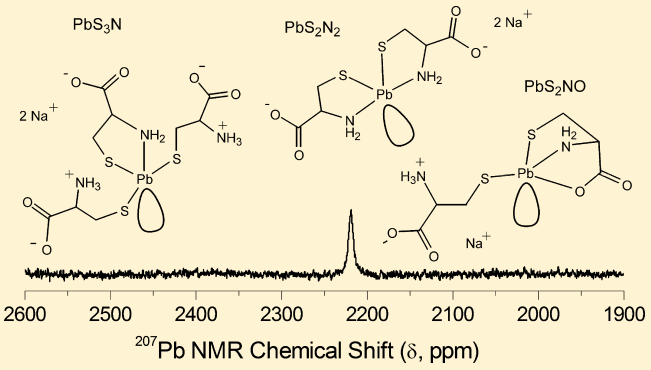

INTRODUCTION

The efficiency of cysteine-rich proteins and peptides, e.g., metallothioneins and phytochelatins, in removing harmful heavy metals from the cells and tissues[1,2] has inspired the assessment of cysteine as an ecofriendly agent for extracting heavy metals from a contaminated environment. Cysteine (H_2Cys = $HSCH_2CH(NH_3^+)COO^-$), as well as penicillamine (H_2Pen) and glutathione (GSH), can liberate lead bound in contaminated soil, in iron/manganese oxides, and in lead phosphate/carbonate salts or in mine tailings by increasing its solubility and mobilization.[3−5] Moreover, the ability of cysteine to capture heavy metals including lead from polluted water can be important in the development of new materials with potential use in drainage and wastewater treatment.[6] A cysteine-based nanosized chelating agent that selectively removes Pb^{II} ions has recently been developed for the treatment of lead poisoning.[7]

In recent years, cysteine has been introduced as an environmentally friendly source of sulfur for preparing nanocrystalline PbS, a widely used semiconductor. Such nanocrystals can be prepared by mixing $Pb(NO_3)_2$ or $Pb(OAc)_2$ (OAc^- = acetate) with cysteine to form a lead(II) cysteine precursor, followed by hydrothermal decomposition to PbS. Different morphologies, shapes, and sizes can be obtained depending on the metal-to-ligand mole ratio, concentration, or pH.[8−11] It has been suggested that the precursor is polycrystalline $HSCH_2CH(NH_2)COOPbOH$[8] or has a polymeric $[-SCH_2CH(COOH)NHPb-]_n$ structure,[11] in well-aligned one-dimensional nanowires.[12]

Corrie and co-workers have reported formation constants for several mononuclear lead(II) cysteine complexes in aqueous solution, including $Pb(Cys)$, $Pb(Cys)_2^{2-}$, $Pb(Cys)_3^{4-}$, $Pb(HCys)^+$, $Pb(Cys)(HCys)^-$, and $Pb(Cys)_2(OH)^{3-}$, however, with revised values, e.g., for the $Pb(Cys)$ complex in their later reports.[13−15] Bizri and co-workers also reported formation constants for the above complexes, except for $Pb(Cys)_3^{4-}$ and $Pb(Cys)_2(OH)^{3-}$, but included a $Pb(Cys)(OH)^-$ complex; see Figure S-1a in the Supporting Information (SI).[16] To explain the high stability of the $Pb(Cys)$ complex, cysteinate was proposed to act as a tridentate ligand, binding simultaneously through the thiolate ($-S^-$), carboxylate ($-COO^-$), and amine ($-NH_2$) groups.[15−17] However, a subsequent study of the COO^- stretching frequencies indicated that cysteinate in an alkaline solution exclusively binds to Pb^{II} via the amine and thiolate groups.[18] Pardo et al. proposed formation constants for

Received: October 22, 2014
Published: February 19, 2015

© 2015 American Chemical Society

DOI: 10.1021/ic5025668
Inorg. Chem. 2015, 54, 2160−2170

a set consisting of the Pb(Cys), $Pb(HCys)^+$, $Pb(HCys)_2$, $Pb(Cys)(HCys)^-$, and $Pb(Cys)_2^{2-}$ complexes.[19] Recently, Crea et al. obtained formation constants for Pb(Cys), $Pb(HCys)^+$, $Pb(H_2Cys)^{2+}$, $Pb(Cys)(OH)^-$, and $Pb(Cys)_2^{2-}$ to describe the stoichiometric composition of the lead(II) cysteine complexes formed at several ionic strengths ($0 < I \leq 1.0$ M $NaNO_3$) and temperatures; see Figure S-2a in the SI.[20] The highest Pb^{II} concentration used in all studies above was 0.5 mM.

In a high-field ^1H and ^{13}C NMR study, Kane-Maguire and Riley investigated the Pb^{II} binding to cysteine at both acidic (pD 1.9) and alkaline (pD 12.9) D_2O solutions.[21] The report includes proton-coupling constants for free cysteine (L), as well as mole fractions of its three rotamers: trans (*t*) and gauche (*g* and *h*), at different pD values in the range 1.80−12.92 (pD = pH reading + 0.4).[21,22] Each rotamer was ascribed a preferred mode of binding: rotamer *t* to bidentate (*S,N*), *h* to tridentate (*S, N, O*), and *g* to bidentate (*S,O*). No significant lead(II) cysteine complex formation was observed in the acidic solutions (pD 1.9) with H_2Cys/Pb^{II} mole ratios 0.5−6.0, which is consistent with the well-known ability of lead(II) to form nitrate complexes.[23] At $H_2Cys/Pb(NO_3)_2$ mole ratios ≥2.0 ($C_{Pb^{II}}$ = 10 mM), only PbL_2 complexes were proposed to form in alkaline media (pD 12.9), with cysteine mainly acting as a tridentate (*S,N,O*) or a bidentate (*S,N*) ligand. It was also suggested that when $C_{Pb(NO_3)_2} = C_{H_2Cys}$ = 10 mM (pD 12.9), PbL species with 63% Pb(*S,N,O*-Cys), 30% Pb(*S,O*-Cys), and 7% Pb(*S,N*-Cys) coordination were formed in proportion to the mole fractions of *h*, *g*, and *t* rotamers, respectively. However, we could not prepare aqueous solutions with 1:1 Pb^{II}/cysteine composition because the initially formed precipitate did not dissolve in alkaline media even at pH 12.0, and stability constants for lead(II) hydrolysis indicate that precipitation of lead(II) hydroxide should start in such highly alkaline media;[20] see Figures S-1b and S-2b in the SI.

Reliable structural information to allow a better understanding of the nature of the lead(II) complexes formed with cysteine is clearly needed. We used a combination of spectroscopic techniques, including UV−vis, ^{207}Pb, ^{13}C, and ^1H NMR, extended X-ray absorption fine structure (EXAFS), and electrospray ion mass spectrometry (ESI-MS) to study the coordination and bonding in lead(II) cysteine complexes formed in two sets of alkaline solutions with $C_{Pb^{II}}$ = 10 and 100 mM for H_2Cys/Pb^{II} mole ratios ≥2.1. To obtain such concentrations, the pH was raised (9.1−10.4) to dissolve the lead(II) cysteine precipitate that forms when adding lead(II) to cysteine solutions. Both the −SH and $-NH_3^+$ groups of cysteine deprotonate at about pH 8.5,[24] thus increasing its ability to coordinate via the thiolate and amine groups.

EXPERIMENTAL SECTION

Sample Preparation. L-Cysteine, cysteamine (Haet, $H_2NCH_2CH_2SH$), PbO, $Pb(ClO_4)_2{\cdot}3H_2O$, and sodium hydroxide were used as supplied (Sigma-Aldrich). All syntheses were carried out under a stream of argon gas. Deoxygenated water for sample preparation was prepared by bubbling argon gas through boiled distilled water. The pH values of the solutions were monitored with a Thermo Scientific Orion Star pH meter.

Two sets of lead(II) cysteine solutions were prepared with different $H_2Cys/Pb(ClO_4)_2$ mole ratios for $C_{Pb^{II}} \sim 10$ and 100 mM, respectively, at an alkaline pH at which the lead(II) cysteine precipitate dissolved; see Table 1. Lead(II) cysteine solutions A−G ($C_{Pb^{II}} \approx 10$ mM) and A*−F* ($C_{Pb^{II}} \approx 100$ mM) were freshly prepared by adding $Pb(ClO_4)_2{\cdot}3H_2O$ (0.05 mmol) to cysteine dissolved in deoxygenated water (0.105−0.75 mmol, pH 2.0−2.4). For ^{207}Pb NMR and UV−vis measurements of solutions A−G, 50 mM stock solutions of enriched ^{207}PbO (94.5%) from Cambridge Isotope Laboratories and PbO dissolved in 0.15 M $HClO_4$ were prepared, respectively. Upon the dropwise addition of 6.0 M NaOH, an off-white precipitate formed, which momentarily dissolved at pH ∼7; after a few seconds, a cream-colored precipitate appeared. The addition of a 1.0 M sodium hydroxide solution continued until the solid dissolved above pH 8.5 and gave a clear colorless solution. For solutions A ($C_{Pb^{II}}$ = 10 mM) and A* ($C_{Pb^{II}}$ = 100 mM), with the mole ratio H_2Cys/Pb^{II} = 2.1, the solid dissolved completely at pH ∼10.4, and for solutions B and B* (H_2Cys/Pb^{II} mole ratio = 3.0), it dissolved at pH 9.1. For consistency, the pH values of solutions with higher H_2Cys/Pb^{II} mole ratios were also set at pH 9.1. The final volume for each solution was adjusted to 5.0 mL. Solutions A−F were used for ESI-MS and ^1H and ^{13}C NMR (prepared in 99.9% deoxygenated D_2O) measurements. For solutions in D_2O, the pH-meter reading was 10.4 for solution A (pD = pH reading + 0.4)[22] and 9.1 for B−F. ^{207}Pb NMR spectra were measured for all solutions (10% v/v D_2O), while Pb L_{III}-edge EXAFS spectra were measured for solutions A−E and A*−F*.

Table 1. Composition of Lead(II) Cysteine Solutions

H_2Cys/Pb^{II} mole ratio	pH	solution	$C_{Pb^{II}}$ (mM)	solution	$C_{Pb^{II}}$ (mM)
2.1	10.4	A	10	A*	100
3.0	9.1	B	10	B*	100
4.0	9.1	C	10	C*	100
5.0	9.1	D	10	D*	100
8.0	9.1	E	10	E*	100
10.0	9.1	F	10	F*	100
15.0	9.1	G	10		
15.0	8.9	G′	10		

Bis(2-aminoethanethiolato)lead(II) Solid, Pb(aet)$_2$. A total of 0.964 g (12.5 mmol) of Haet dissolved in 10 mL of deoxygenated water (pH 9.6) was added to a suspension of PbO (1.116 g, 5 mmol) in 50 mL of ethanol at 50 °C and refluxed for 3 h under an argon atmosphere, giving a pale-yellow solution, which was then filtered and cooled in a refrigerator. Colorless crystals formed after 48 h and were filtered, washed with ethanol, and dried under vacuum (turning yellow). Eleme anal. Calcd for $Pb(SCH_2CH_2NH_2)_2$: C, 13.36; H, 3.37; N, 7.79. Found: C, 13.41; H, 3.43; N, 7.81. The unit cell dimensions of the crystal were also verified, matching the literature values.[25]

Methods. Details about instrumentation and related procedures for ESI-MS (Aglient 6520 Q-Tof), UV−vis (Cary 300), and ^1H, ^{13}C, and ^{207}Pb NMR spectroscopy (Bruker AMX 300 and Avance II 400 MHz), as well as EXAFS data collection and data analyses are provided elsewhere.[26] UV−vis spectra of solutions A−G were measured using 0.25, 0.5, and 0.75 nm data intervals, with a 1.5 absorbance Agilent rear-beam attenuator mesh filter in the reference position. ESI-MS spectra for solutions A, B, and F were measured in both positive- and negative-ion modes. ^{207}Pb NMR spectra for solutions A−G enriched in ^{207}Pb were measured at room temperature using a Bruker AMX 300 equipped with a 10 mm broad-band probe. For these solutions, the ^{207}Pb NMR chemical shift was externally calibrated relative to 1.0 M $Pb(NO_3)_2$ in D_2O, resonating at −2961.2 ppm relative to $Pb(CH_3)_4$ (δ = 0 ppm).[27] Approximately 12800−51200 scans for ^{207}Pb NMR, 16−32 scans for ^1H NMR, and 500−3000 scans for ^{13}C NMR were coadded for the solutions. One-pulse magic-angle-spinning (MAS) ^{207}Pb NMR spectra for crystalline $Pb(aet)_2$ were acquired with high-power proton decoupling on an AVANCE III 200 NMR spectrometer at room temperature (^{207}Pb, 41.94 MHz). Ground crystals were packed in a 7 mm zirconia rotor, spinning at MAS rates of 5.8 and 5.5 kHz using 800 and 895 scans, respectively, with a 5.0 s recycle delay. Chemical shifts were referenced relative to $Pb(CH_3)_4$, by setting the ^{207}Pb NMR peak of solid $Pb(NO_3)_2$ spinning at a 1.7 kHz rate at −3507.6 ppm (295.8 K).[28,29] Static ^{207}Pb NMR powder patterns were reconstructed by iteratively fitting the sideband manifold using the *Solids Analysis* package within Bruker's *TOPSPIN 3.2* software.

DOI: 10.1021/ic5025668
Inorg. Chem. 2015, 54, 2160−2170

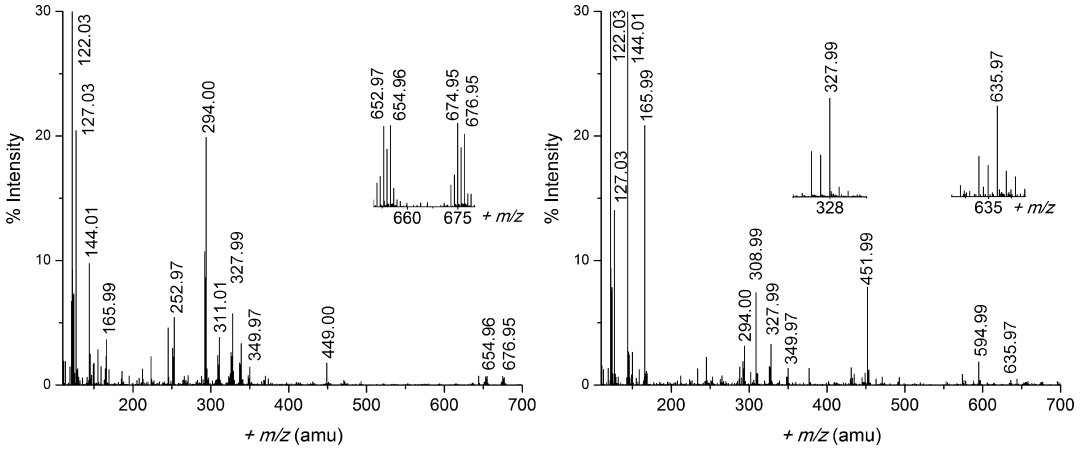

Figure 1. ESI-MS spectra measured in positive-ion mode for solutions A (left) and F (right) ($C_{Pb^{II}}$ = 10 mM) with H_2Cys/Pb^{II} mole ratios 2.1 and 10.0, respectively. The peak at 122.03 amu has 100% intensity. Selected peaks assigned to lead(II) species with distinct isotopic patterns for Pb are shown in the inset.

Pb L_{III}-edge X-ray absorption spectroscopy (XAS) spectra were measured at ambient temperature at the Stanford Synchrotron Radiation Lightsource (SSRL) for freshly prepared solutions A–E and A* at BL 7-3 (500 mA; equipped with a rhodium-coated harmonic rejection mirror) and for solutions B*–F* at BL 2-3 (100 mA). A double-crystal monochromator with Si(220) was used at both beamlines. To remove higher harmonics, the monochromator was detuned to eliminate 50% of the maximum intensity of the incident beam (I_0) at the end of the scan at BL 2-3. To avoid photoreduction of the samples at BL 7-3, the beam size was adjusted to 1 × 1 mm, and the intensity of the incident beam was reduced to 80% of the maximum of I_0 at 13806 eV. A high beam intensity could result in precipitation of a small amount of black particles in the sample holder, especially in solutions containing excess ligand. For solutions containing $C_{Pb^{II}}$ = 10 mM, 12–13 scans were measured in both transmission and fluorescence modes, detecting X-ray fluorescence using a 30-channel germanium detector, while for the more concentrated solutions with $C_{Pb^{II}}$ = 100 mM between three and four scans were collected in transmission mode. For each sample, consecutive scans were averaged after comparison to ensure that no radiation damage had occurred. The energy scale was internally calibrated by assigning the first inflection point of a lead foil at 13035.0 eV. The threshold energy E_0 in the XAS spectra of the lead(II) cysteine solutions varied within a narrow range: 13034.0–13034.9 eV. Least-squares curve fitting of the EXAFS spectra was performed for solutions A, B, A*, B*, and F* over the k range = 2.7–11.7 $Å^{-1}$, using the D-penicillaminatolead(II) (PbPen) crystal structure[30] as the model in the *FEFF 7.0* program.[31,32] For each scattering path, the refined structural parameters were the bond distance (R), the Debye–Waller parameter (σ^2), and in some cases the coordination number (N). The amplitude reduction factor (S_0^2) was fixed at 0.9 (obtained from EXAFS data analysis of solid PbPen),[33] while ΔE_0 was refined as a common value for all scattering paths. The accuracy of the Pb–(N/O) and Pb–S bond distances and the corresponding Debye–Waller parameters is within ±0.04 Å and ±0.002 $Å^2$, respectively. Further technical details about EXAFS data collection and data analyses were provided previously.[26]

Principal component analysis (PCA), introduced in the *EXAFSPAK* suite of programs,[34] was applied on the raw k^3-weighted experimental EXAFS spectra for solutions A–E and A*–F* over the k range of 2.7–11.7 $Å^{-1}$. *DATFIT*, another program in the *EXAFSPAK* package, was used to fit the k^3-weighted EXAFS spectra of lead(II) cysteine solutions A–E and A*–F* to a linear combination of EXAFS oscillations for species with $PbS_2N(N/O)$, PbS_3N, and PbS_3 coordination to estimate the amount of such species in each lead(II) cysteine solution. For the PbS_3N model, theoretical EXAFS oscillations were simulated by stepwise variation of the Pb–S and Pb–N parameters: Pb–S 2.67–2.70 Å [using σ^2 = 0.0065 $Å^2$ from EXAFS least-squares refinement of lead(II) glutathione solutions with excess ligand],[33] Pb–N 2.40–2.43 Å (σ^2 = 0.004, 0.006, and 0.008 $Å^2$), and S_0^2 = 0.9. The best fits were obtained for Pb–S = 2.68 Å (σ^2 = 0.0065 $Å^2$) and Pb–N = 2.40 Å (σ^2 = 0.0080 $Å^2$).

RESULTS

ESI-MS. ESI-MS spectra were measured in both positive- and negative-ion modes for the lead(II) cysteine solutions A, B, and F, with $C_{Pb^{II}}$ = 10 mM and H_2Cys/Pb^{II} mole ratios 2.1, 3.0, and 10.0, respectively, as shown in Figures 1 and S-3 in the SI, to identify possible charged lead(II) cysteine complexes. The assignment of the mass ions, presented in Tables 2 and S-1 in the SI, is facilitated by the distinct isotopic distribution pattern for lead(II) species due to the natural abundance of 52.4% ^{208}Pb, 22.1% ^{207}Pb, 24.1% ^{206}Pb, and 1.4% ^{204}Pb.[35] The ESI-MS spectra for solutions A and B were nearly identical, showing positive-ion mass peaks for species with metal-to-ligand mole ratios 1:1, 1:2, and 2:2. Such mass peaks were also previously detected for a 1:1 mixture of $Pb(NO_3)_2$ and cysteine in 50% methanol/water and considered to be independent of the reaction mixture stoichiometry (1:10 or 10:1).[36] We could also detect a 1:3 species $[3Na^+ + Pb(H_2Cys)_3 - 4H^+]^+$ at 635.97

Table 2. Assignment of Mass Ions Observed in ESI-MS Spectra (Positive-Ion Mode) for Lead(II) Cysteine Solutions A, B, and F ($C_{Pb^{II}}$ = 10 mM; H_2Cys/Pb^{II} Mole Ratios 2.1, 3.0, and 10.0, Respectively)[a]

m/z (amu)	assignment	m/z (amu)	assignment
122.03	$[H_2Cys + H^+]^+$	327.99	$[Pb(H_2Cys) - H^+]^+$
144.01	$[Na^+ + H_2Cys]^+$	349.97	$[Na^+ + Pb(H_2Cys) - 2H^+]^+$
165.99	$[2Na^+ + H_2Cys - H^+]^+$	449.00	$[Pb(H_2Cys)_2 - H^+]^+$
252.97	$[Pb(HCOO)]^+$	451.99	$[4Na^+ + 3(H_2Cys) - 3H^+]^+$
294.00	$[Pb(H_2Cys) - H^+ - H_2S]^+$	594.99	$[5Na^+ + 4(H_2Cys) - 4H^+]^+$
308.99	$[3Na^+ + 2(H_2Cys) - 2H^+]^+$	635.97	$[3Na^+ + Pb(H_2Cys)_3 - 4H^+]^+$
311.01	$[PbC_2H_5N_3O_2]^+$	654.96	$[Pb_2(H_2Cys)_2 - 3H^+]^+$
		676.95	$[Na^+ + Pb_2(H_2Cys)_2 - 4H^+]^+$

[a] H_2Cys ($C_3H_7NO_2S$); m/z 121.02.

DOI: 10.1021/ic5025668
Inorg. Chem. 2015, 54, 2160–2170

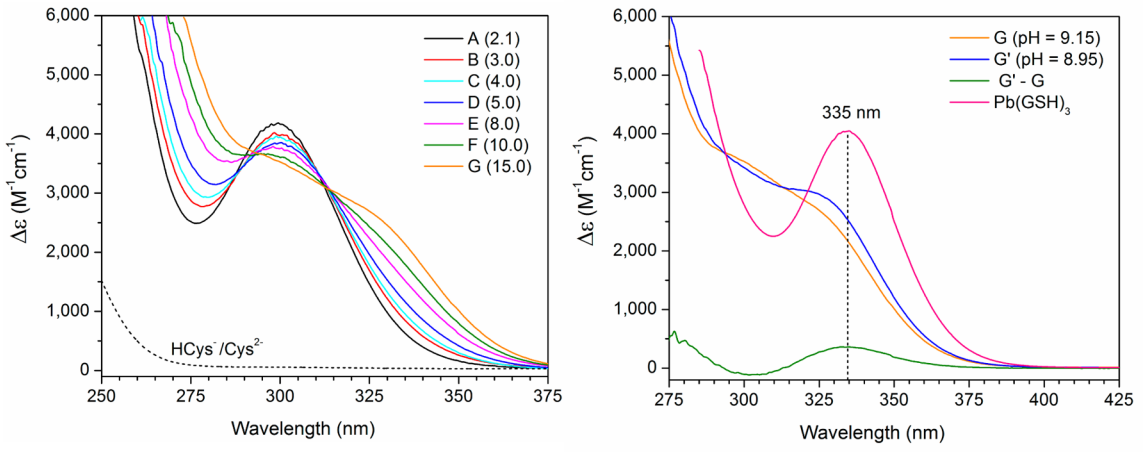

Figure 2. (left) UV–vis spectra of lead(II) cysteine solutions A–G with $C_{Pb^{II}}$ = 10 mM and H_2Cys/Pb^{II} mole ratios 2.1–15.0 compared with that of a 10 mM cysteine solution (dots, pH 9.1). (right) UV–vis spectra of 10 mM lead(II) solutions containing H_2Cys/Pb^{II} mole ratio 15.0 at pH 9.15 (solution G) and at pH 8.95 (solution G′) and their difference (G′ − G) compared with that of a lead(II) glutathione solution with GSH/Pb^{II} mole ratio 10.0 (pH 8.5).[33] Data interval = 0.5 nm.

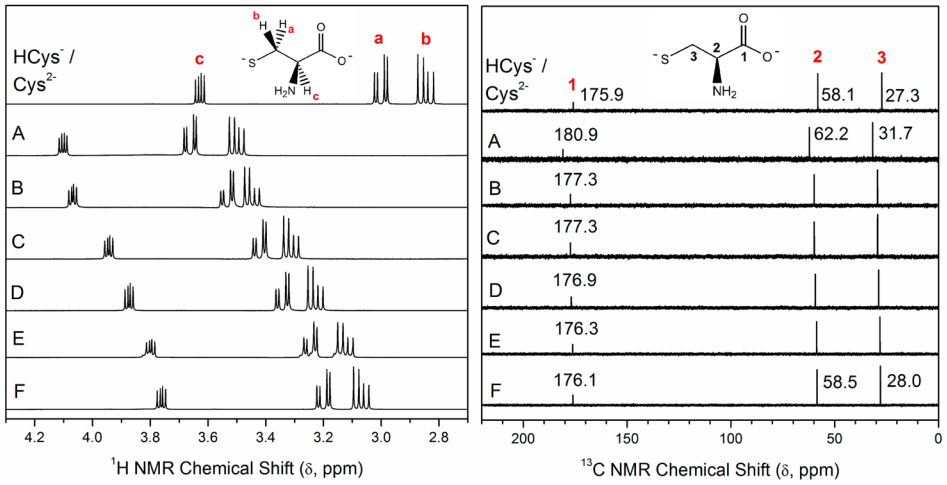

Figure 3. ^1H and ^{13}C NMR spectra of 0.1 M cysteine in D_2O (pH 9.1) and alkaline lead(II) cysteine solutions (99.9% D_2O) with $C_{Pb^{II}}$ = 10 mM and H_2Cys/Pb^{II} mole ratios 2.1 (A), 3.0 (B), 4.0 (C), 5.0 (D), 8.0 (E), and 10.0 (F). See Table 1.

amu in the spectrum of solution F. In negative-ion mode, only one mass peak corresponding to a lead(II) complex was observed, assigned to the $[Pb(H_2Cys)_2 - 3H^+]^-$ ion (446.99 amu).

Electronic Absorption Spectroscopy. Figure 2 (left) displays the UV–vis spectra for the lead(II) cysteine solutions A–G ($C_{Pb^{II}}$ = 10 mM). The absorption bands have been attributed to a combination of S^- 3p → Pb^{II} 6p ligand-to-metal charge-transfer and Pb^{II} intraatomic transitions.[37−40] The peak maximum for solution A, λ_{max} = 298 nm (C_{H_2Cys} = 21 mM; pH 10.4) shows a slight red shift to λ_{max} = 300 nm as the ligand concentration increases in solution B with H_2Cys/Pb^{II} mole ratio 3.0 at pH 9.1 (Figure S-4a in the SI).

For solutions E–G with high free ligand concentration (50–120 mM), a growing shoulder appears around $\lambda \sim 330$ nm, while the intensity of the peak at ~300 nm reduces significantly. This shoulder is blue-shifted relative to the maximum absorption recorded at 335 nm for a lead(II) glutathione solution (pH 8.5) containing excess ligand (Figure 2, right).[33] The amplitude of this shoulder is pH-dependent, as shown in Figure 2 (right) for 10 mM lead(II) solutions containing H_2Cys/Pb^{II} mole ratio 15.0 at pH 9.15 (solution G) and pH 8.95 (solution G′). The difference of these two spectra (G′ − G) shows that when the pH is lowered by 0.2 units, a peak at 335 nm emerges, very similar to λ_{max} in the UV–vis spectrum of the lead(II) glutathione solution.[33] There is no true isosbestic point around 312 nm, as shown in Figure S-4b in the SI by the systematic movement of crossing points of the absorption spectra of solutions B–G with that of solution A.

^1H and ^{13}C NMR Spectroscopy. The ^1H and ^{13}C NMR spectra of a 0.1 M cysteine solution (pH 9.1) and the lead(II) cysteine solutions A–F ($C_{Pb^{II}}$ = 10 mM) prepared in D_2O are shown in Figure 3, with the ^1H NMR chemical shifts (δ_H) shown in Table S-2 in the SI. For lead(II)-containing solutions, only one set of signals was observed for the H_a–H_c and C_1–C_3 atoms in both Pb^{II}-bound and free cysteine because of fast ligand exchange on the NMR time scale. These average resonances were all shifted downfield relative to the corresponding peaks in free cysteine (see Table S-2 in the SI), with the largest shifts ($\Delta\delta$) observed for solution A (H_2Cys/Pb^{II} mole ratio = 2.1), which contains the least amount of free ligand. Satellites originating from ^{207}Pb nuclei were not observed in the ^{13}C NMR spectra.

DOI: 10.1021/ic5025668
Inorg. Chem. 2015, 54, 2160−2170

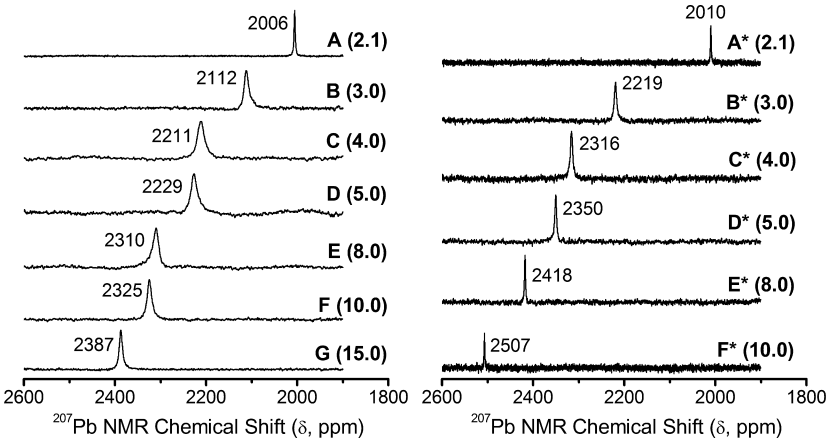

Figure 4. ^{207}Pb NMR spectra of the alkaline aqueous lead(II) cysteine solutions A−G enriched in ^{207}Pb ($C_{Pb^{II}}$ = 10 mM; H_2Cys/Pb^{2+} mole ratios 2.1−15.0) and A*−F* with 10% D_2O ($C_{Pb^{II}}$ = 100 mM; H_2Cys/Pb^{2+} mole ratios 2.1−10.0).

^{207}Pb NMR Spectroscopy. The chemical shift of the ^{207}Pb nucleus spans over a wide range (~17000 ppm). It is sensitive to the local structure and electronic environment, the nature of surrounding donor atoms, the bond covalency, and the coordination number and is affected by the temperature and concentration.[27,28,41−43] We measured ^{207}Pb NMR spectra for two sets of alkaline aqueous lead(II) cysteine solutions (containing 10% D_2O), with increasing H_2Cys/Pb^{II} mole ratios (Table 1). Calculated distribution diagrams based on different sets of stability constants indicate that the dominating lead(II) complexes would be either $[Pb(Cys)_2]^{2-}$ (Figure S-2b in the SI),[20] or a mixture of $[Pb(Cys)_2]^{2-}$ and $[Pb(Cys)(HCys)]^-$ (Figure S-1b in the SI).[16] Figure 4 presents the ^{207}Pb NMR spectra for solutions A−G ($C_{Pb^{II}}$ = 10 mM; enriched in ^{207}Pb) and A*−F* ($C_{Pb^{II}}$ = 100 mM), all with only an average NMR resonance. Solutions A and A*, both with the H_2Cys/Pb^{II} mole ratio = 2.1 at pH 10.4, show sharp signals at 2006 and 2010 ppm, respectively, which are ~184−200 ppm deshielded relative to that of lead(II) penicillamine (3,3′-dimethylcysteine) solutions with similar composition (~1806−1826 ppm).[26] The sharpness of this signal results from fast ligand exchange (in the NMR time scale) between the lead(II) complexes in solution. As the ligand concentration increases in solutions B and B* (H_2Cys/Pb^{II} = 3.0) and the pH changes to 9.1, the ^{207}Pb resonance becomes broader and shifts ~106 (B) and ~209 (B*) ppm downfield and more for the higher ligand concentration. Broad averaged signals indicate ligand exchange between several lead(II) species at intermediate rates. Solution F* containing $C_{Pb^{II}}$ = 100 mM and C_{H_2Cys} = 1.0 M shows the most deshielded ^{207}Pb NMR resonance (2507 ppm), which still is ~286 ppm upfield relative to that of the Pb(*S*-GSH)$_3$ complex (2793 ppm) with PbS_3 coordination.[33]

For comparison, we measured one-pulse MAS ^{207}Pb NMR spectra of the crystalline bis(2-aminoethanethiolato)lead(II) complex, Pb(*S*,*N*-aet)$_2$, at two different spin rates, 5.5 and 5.8 kHz (see Figures 5 and S-5a in the SI), and observed an isotropic chemical shift of δ_{iso} = 2105 ppm for this complex with PbS_2N_2 coordination.[25] Reconstruction of a static ^{207}Pb NMR powder pattern for spin rate 5.8 kHz resulted in the following principal components: δ_{11} = 3707.98 ppm, δ_{22} = 2831.04 ppm, δ_{33} = −223.12 ppm, leading to $\delta_{iso} = 1/3(\delta_{11} + \delta_{22} + \delta_{33})$ = 2105.3 ppm (see Figure S-5b in the SI). The isotropic chemical shift is ~600 ppm upfield relative to the only other ^{207}Pb chemical shift that is reported for PbS_2N_2 coordination, δ_{iso} = 2733 ppm for Pb(2,6-$Me_2C_6H_3S)_2(py)_2$ (py = pyridine). In that lead(II) complex, all ligands are monodentate (i.e., not forming a chelate ring) and pyridine is the N-donor ligand.[44]

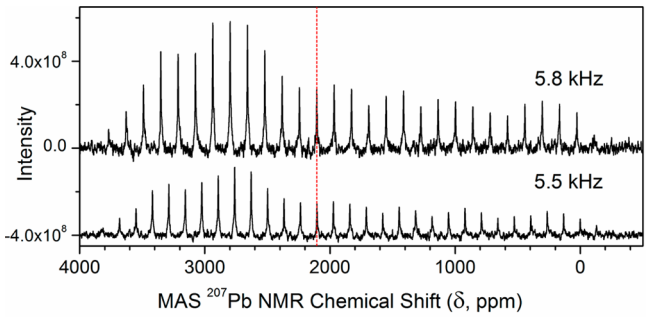

Figure 5. One-pulse proton-decoupled MAS ^{207}Pb NMR spectra of crystalline Pb(*S*,*N*-aet)$_2$, measured at two different spin rates (5.5 and 5.8 kHz) at room temperature. The dashed vertical line shows the isotropic chemical shift δ_{iso} = 2105 ppm (identified from overlapping spectra in Figure S-5a in the SI).

We also obtained the ^{207}Pb NMR spectrum of an aqueous lead(II) cysteamine solution, prepared by dissolving crystalline (mononuclear) Pb(aet)$_2$ in a solution containing the same number of moles of cysteamine, with a final lead(II)/cysteamine mole ratio of 1:3 (10% D_2O; $C_{Pb^{II}}$ ~ 76 mM; pH 10.1). A signal at 2212 ppm was observed (Figure S-6 in the SI), probably from a mixture of mononuclear Pb(*S*,*N*-aet)$_2$ (PbS_2N_2 coordination), $[Pb(S,N\text{-aet})(S\text{-Haet})(OH/OH_2)]^n$ (n = 0, 1; PbS_2NO), and $[Pb(S,N\text{-aet})(S\text{-Haet})_2]^+$ (PbS_3N) complexes. A minor amount of PbS_3N species is a likely reason for the ~100 ppm deshielding of the ^{207}Pb NMR resonance for this solution, relative to the isotropic chemical shift of crystalline Pb(aet)$_2$ (δ_{iso} = 2105 ppm). Moreover, multinuclear species such as the $[Pb_2(aet)_3]^+$ complex may form,[45] where Pb^{II} ions can adopt PbS_3N coordination through bridging thiolate groups. However, Li and Martell could only identify mononuclear $[Pb(Haet)]^{2+}$, $[Pb(aet)]^+$, and Pb(aet)(OH) complexes in dilute solutions with $C_{Pb^{II}}$ = 1.0 mM (C_{Haet} = 1.0−2.0 mM; pH 2−8).[46]

Pb L_{III}-Edge XAS. The near-edge features in the XAS spectra are nearly identical for the lead(II) cysteine solutions, as shown in Figure S-7 in the SI, and are evidently not sensitive to the changes in lead(II) speciation as the ligand concentration

DOI: 10.1021/ic5025668
Inorg. Chem. 2015, 54, 2160−2170

increases. When the extended regions are compared, the EXAFS spectra and corresponding Fourier transforms are also quite similar for solutions A, B, and E in the $C_{Pb^{II}}$ = 10 mM series (Figure S-8 in the SI), while for solutions A*−F* ($C_{Pb^{II}}$ = 100 mM), the amplitude of the EXAFS oscillation (and the Fourier transform) shows a gradual increase as the total concentration of cysteine increases from 0.21 to 1.0 M (Figure S-8 in the SI). The k^3-weighted EXAFS spectrum of the lead(II) cysteine solution A* (C_{H_2Cys} = 210 mM; pH 10.4) closely overlaps with that of a lead(II) penicillamine aqueous solution ($C_{Pb^{II}}$ = 100 mM; H_2Pen/Pb^{II} = 3.0; pH 9.6), in which the dithiolate $[Pb(S,N,O\text{-Pen})(S\text{-}H_nPen)]^{2-n}$ (n = 0−1) species dominates;[26] see Figure S-9 in the SI.

PCA of the raw k^3-weighted EXAFS spectra of the six lead(II) cysteine aqueous solutions A*−F* and of the five solutions A−E displayed two major components with clear oscillatory patterns (Figure S-10, top, in the SI). Using *TARGET* in the *EXAFSPAK* package on the PCA output file showed that two of the PCA components in each series matched fairly well with the raw k^3-weighted EXAFS oscillations obtained experimentally for 0.1 M lead(II) solutions containing penicillamine (C_{H_2Pen} = 0.3 M; pH 9.6) or *N*-acetylcysteine (C_{H_2NAC} = 1.0 M; pH 9.1). These solutions are dominated by PbS_2NO and PbS_3 species, respectively.[26,47] In the next step, the *DATFIT* program in the *EXAFSPAK* suite was used to estimate the relative amounts of such $PbS_2N(N/O)$- and PbS_3-coordinated species in the lead(II) cysteine solutions A*−F*. This was achieved by fitting the k^3-weighted EXAFS spectra of solutions A*−F* to a linear combination of EXAFS oscillations for the lead(II) penicillamine/*N*-acetylcysteine solutions; however, a clear oscillatory residual was observed. That residual amplitude increased when fitting the EXAFS spectra of solutions with higher H_2Cys/Pb^{II} mole ratios; see Figure S-11a in the SI, indicating a substantial additional contribution from another lead(II) species (or scattering path), probably a four-coordinated PbS_3N complex. Note that coordinated O and N atoms cannot be distinguished by EXAFS spectroscopy, and the $PbS_2N(N/O)$ and PbS_3N coordination modes used here are based on the interpretation of ^{207}Pb NMR spectra (see the Discussion section).

EXAFS oscillations were then theoretically simulated for a PbS_3N model using the *WinXAS*[48] and *FEFF 7.0* programs, varying the Pb−S and Pb−N parameters stepwise within reasonable ranges and keeping S_0^2 = 0.9 (see the Methods section). The best fits with considerably smaller residuals were obtained when including the simulated EXAFS oscillation for this model in the linear combination, considering Pb−S 2.68 Å (σ^2 = 0.0065 Å^2) and Pb−N 2.40 Å (σ^2 = 0.0080 Å^2); see Figure S-11b in the SI. These fittings clearly show that di- and trithiolate lead(II) complexes with $PbS_2N(N/O)$ and PbS_3N coordination give major contributions to the EXAFS spectra of the lead(II) cysteine solutions A*−F* (Table 3). Including the PbS_3-coordinated model in the fitting only slightly improved the residual (Figure S-11c in the SI), indicating a minor and uncertain contribution (Table S-3 in the SI), especially because there are only two major oscillatory PCA components (Figure S-10 in the SI, top). Although the EXAFS spectra of solutions E* and F* nearly overlap (Figure S-8 in the SI), the percentages of PbS_3N/PbS_3 from their linear combination fitting results vary about ±10%. Similarly, the PbS_3 contribution in the EXAFS spectra of solutions A−E is also minor and uncertain (Figure S-11e and Table S-3 in the SI). The fittings of

Table 3. Results of Fitting the Raw k^3-Weighted Pb L_{III}-Edge EXAFS Spectra of Lead(II) Cysteine Solutions A*−F* and A−E with Linear Combinations of EXAFS Oscillations for $PbS_2N(N/O)$ and PbS_3N Models (See the Text; Figures S-11b and S-11d in the SI)[a]

solution (H_2Cys/Pb^{II} mole ratio)	$\delta(^{207}Pb)$ (ppm)	$PbS_2NO + PbS_2N_2$ (%)	PbS_3N (%)
A (2.1)	2006	89	11
B (3.0)	2112	80	20
D (5.0)	2229	74	26
E (8.0)	2310	73	27
A* (2.1)	2010	91	9
B* (3.0)	2219	77	23
C* (4.0)	2316	69	31
D* (5.0)	2350	63	37
E* (8.0)	2418	60	40
F* (10.0)	2507	51	49

[a]The raw k^3-weighted EXAFS spectrum of a 0.1 M lead(II) penicillamine solution (C_{H_2Pen} = 0.3 M; pH 9.6) was used for the $PbS_2N(N/O)$ model. The EXAFS oscillation for PbS_3N was theoretically simulated (see the text). The estimated error limit of the relative amounts is ±10−15%. For the results when including the PbS_3 contribution in the fitting, see Table S-3 in the SI.

linear combinations of EXAFS oscillations for the $PbS_2N(N/O)$ and PbS_3N models to the EXAFS spectra of the dilute lead(II) cysteine solutions A−E ($C_{Pb^{II}}$ = 10 mM) are shown in Figure S-11d in the SI, with results in Table 3.

Least-squares curve fitting of the EXAFS spectra obtained for lead(II) cysteine solutions only provides an average of the bond distances around the Pb^{II} ions in the above species. Thus, a coordination model comprising the Pb−(N/O) and Pb−S paths was used to simulate the theoretical EXAFS oscillation, which was fitted to the extracted EXAFS spectra for the lead(II) cysteine solutions A, A* and B, B*, with H_2Cys/Pb^{II} mole ratios 2.1 and 3.0, respectively, for which $\delta(^{207}Pb) \sim 2000-2220$ ppm was observed. The curve-fitting results are displayed in Figure 6, with corresponding structural parameters in Table 4. The average Pb-(N/O) and Pb−S bond distances were 2.42

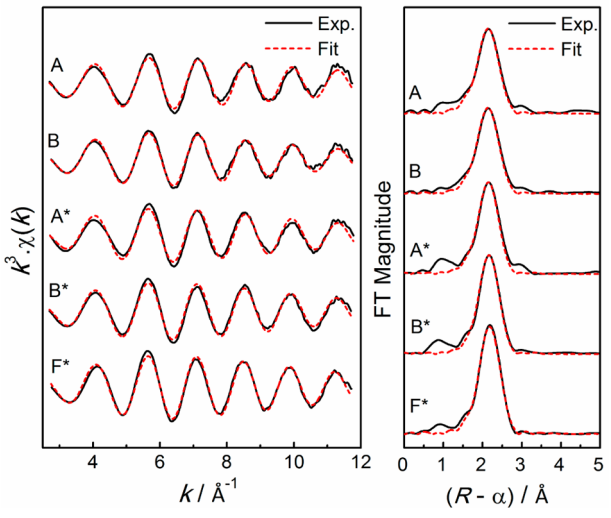

Figure 6. Least-squares curve fitting of k^3-weighted Pb L_{III}-edge EXAFS spectra and corresponding Fourier transforms for lead(II) cysteine solutions A and B ($C_{Pb^{II}}$ = 10 mM) and A*−F* ($C_{Pb^{II}}$ = 100 mM) with different H_2Cys/Pb^{II} mole ratios (see Table 4).

DOI: 10.1021/ic5025668
Inorg. Chem. 2015, 54, 2160−2170

± 0.04 and 2.64 ± 0.04 Å, respectively, with corresponding Debye–Waller parameters varying over the ranges σ^2 = 0.014–0.024 and 0.0043–0.0061 Å^2, respectively. Attempts to resolve two different Pb–(N/O) distances resulted in one quite short (2.33 Å) and another fairly long (2.50 Å) distances; see model III in Table S-4 in the SI. The shortest Pb–N distance found in crystal structures with PbS_2N_2 coordination is 2.401 Å (Cambridge Structural Database code: NOGQOQ), and the shortest recorded Pb–O distance in crystalline PbS_2O_2 complexes is 2.349 Å (CSD code: ZOXGAU).[33,49]

Table 4. Structural Parameters Obtained from Least-Squares Curve Fitting of Pb L_{III}-Edge EXAFS Spectra of Lead(II) Cysteine Solutions (See Figure 6)[a]

solution (H_2Cys/Pb^{II} mole ratio)	Pb–(N/O)			Pb–S		
	N	R (Å)	σ^2 (Å^2)	N	R (Å)	σ^2 (Å^2)
A (2.1)	2*f*	2.40	0.014	1.6	2.64	0.0043
B (3.0)	2*f*	2.43	0.016	2.0	2.64	0.0061
A* (2.1)	2*f*	2.42	0.020	2.0	2.64	0.0055
B* (3.0)	2*f*	2.43	0.024	2.3	2.65	0.0059
F* (10.0)[b]	1.5*f*	2.43	0.0185	2.5*f*	2.66	0.0055

[a] S_0^2 = 0.9 fixed; *f* = fixed value; R ± 0.04 Å; σ^2 ± 0.002 Å^2. [b] Assuming 50:50% PbS_2N(N/O) and PbS_3N coordination environments.

Solutions E* and F* with high free ligand concentration ($C_{Pb^{II}}$ = 100 mM; C_{H_2Cys} = 0.8–1.0 M) and overlapping EXAFS spectra (Figure S-8 in the SI) contain a significant amount of trithiolate species, as evidenced by the considerable downfield shift of their ^{207}Pb NMR signals (Figure 4), as well as the linear combination fitting of the EXAFS spectra (Figure S-11b in the SI). A 50:50% mixture of PbS_2N(N/O) and PbS_3N species would correspond to 1.5 Pb–(N/O) and 2.5 Pb–S path frequencies (N). Fitting the EXAFS spectra of solution F* with such a model led to a slightly longer average Pb–S distance, 2.66 ± 0.04 Å, than those for solutions A* and B* with lower free ligand concentration (Tables 4 and S-4 in the SI).

DISCUSSION

The sets of stability constants for lead(II) cysteine complexes obtained at low concentrations ($C_{Pb^{II}} \leq$ 0.5 mM) reported by Bizri et al. (ionic strength I = 1.0 M) and Crea et al. ($0 < I \leq$ 1.0 M),[16,20] show mixtures of monomeric PbCys, Pb(OH)-(Cys)$^-$, $Pb(Cys)_2^{2-}$, and/or Pb(HCys)(Cys)$^-$ species in alkaline solutions (Figures S-1a and S-2a in the SI). At higher concentrations, such as in the current study, PbCys(c) precipitates within a wide pH range.[18,50,51] Because no solubility product is available for this solid compound, we estimated a solubility product that approximately matched its observed dissolution at alkaline pH (see Table 1): log K_{sp} = −15.2 and −16.2 for the two sets, respectively. The fraction diagrams in Figures S-1b and S-2b in the SI, based on the reported stability constants, are then assumed to approximately account for the distribution of lead(II) cysteine species at $C_{Pb^{II}}$ = 10 or 100 mM with different H_2Cys/Pb^{II} mole ratios.

Solutions with H_2Cys/Pb^{II} = 2.1 (pH 10.4). According to the fraction diagrams in Figures S-1b and S-2b in the SI, the $[Pb(Cys)_2]^{2-}$ complex would dominate in the alkaline aqueous solution A ($C_{Pb^{II}}$ = 10 mM), with minor amounts of $[Pb(Cys)(OH)]^-$ and/or $[Pb(HCys)(Cys)]^-$ species present.

The ESI-MS spectra of solution A showed peaks in the positive-ion mode corresponding to the 1:1, 1:2, and 2:2 species $[Pb(HCys)]^+$, $[Pb(H_2Cys)_2 - H^+]^+$, and $[Pb_2(H_2Cys)_2 - 3H^+]^+$ mass ions, respectively, and in the negative-ion mode to the $[Pb(H_2Cys)_2 - 3H^+]^-$ ion (Figure 1 and Table 2). In the ^{13}C NMR spectrum of solution A, the carboxylate COO^- group showed the highest change in the chemical shift $\Delta\delta$ (^{13}C) relative to free cysteine (Figure 3 and Table S-2 in the SI), indicating that it is bound to the Pb^{II} ion. The change in $\Delta\delta$(^{13}C) for this solution (5.0 ppm) is slightly smaller than that of the corresponding lead(II) penicillamine solution (6.0 ppm),[26] probably because in a mixture of Pb^{II} bound to tridentate (*S,N,O*-Cys^{2-}) and bidentate (*S,N*-Cys^{2-}) cysteinate ligands, the cysteine COO^- group is less involved in Pb^{II} bonding than the tridentate penicillaminate (*S,N,O*-Pen^{2-}) ligand.

The ^{207}Pb NMR signals for solutions A and A* ($C_{Pb^{II}}$ = 100 mM), both with mole ratio H_2Cys/Pb^{II} = 2.1, appeared at δ_{Pb} = 2006 and 2010 ppm, respectively (Figure 4). These chemical shifts are more shielded than the isotropic chemical shift of Pb(*S,N*-aet)$_2$ (δ_{iso} = 2105 ppm) with PbS_2N_2 coordination (Figure 5) and deshielded relative to the recorded chemical shifts for similar lead(II) penicillamine solutions with PbS_2NO coordination (δ_{Pb} = 1806–1826 ppm).[26] The above results indicate that solutions A and A* are dominated by a mixture of $[Pb(S,N,O\text{-Cys})(S\text{-HCys})]^-$ and $[Pb(S,N\text{-Cys})_2]^{2-}$ complexes, consistent with the fraction diagrams for mole ratio H_2Cys/Pb^{II} = 2.1 in Figure S-1b in the SI, which are in fast ligand exchange in the NMR time scale, resulting in an average signal in their ^{1}H, ^{13}C, and ^{207}Pb NMR spectra. Assuming that these two complexes are the only species present in solutions A and A* and that the shift in the ^{207}Pb NMR signal is proportional to the percentages of PbS_2N_2 (isotopic δ_{Pb} = 2105 ppm) and PbS_2NO (δ_{Pb} = 1870 ppm) coordination under similar experimental conditions, the amount of these complexes can be estimated to approximately ~60% $[Pb(S,N\text{-Cys})_2]^{2-}$ and ~40% $[Pb(S,N,O\text{-Cys})(S\text{-HCys})]^-$.

Although the main fraction of Pb^{II} in solution A is present as $[Pb(S,N\text{-Cys})_2]^{2-}$, the UV–vis spectrum of this solution shows the same λ_{max} (298 nm) as a lead(II) penicillamine solution (H_2Pen/Pb^{II} mole ratio 3.0; pH 9.6) with $[Pb(S,N,O\text{-Pen})(S\text{-HPen})]^-$ as the single dominating species (Figure S-4a, left, in the SI).[26] Therefore, the above two dithiolate lead(II) cysteine complexes with PbS_2NO and PbS_2N_2 coordination cannot be easily distinguished via their UV–vis absorption.

Least-squares curve fitting of the EXAFS oscillations for solutions A and A* resulted in average Pb–S and Pb–(N/O) distances of 2.64 ± 0.04 and 2.41 ± 0.04 Å, respectively (Table 4). The high Debye–Waller parameter σ^2 = 0.014–0.02 Å^2 of the Pb–(N/O) path describes a large variation around the mean distance. The average Pb–S distance obtained for these solutions is between those obtained from EXAFS curve fitting of crystalline Pb(aet)$_2$ (2.62 ± 0.02 Å; Table S-5 and Figure S-12 in the SI) and PbPen (2.68 ± 0.04 Å).[33] The mean Pb–(N/O) distance is considerably shorter than the average Pb–N distance (2.54 ± 0.04 Å) refined for Pb(aet)$_2$ (Table S-5 in the SI) and is close to the average Pb–(N/O) bond length obtained from EXAFS analysis of the PbPen compound (2.42 ± 0.04 Å; σ^2 = 0.013 ± 0.002 Å^2).[33]

Solutions with H_2Cys/Pb^{II} = 3.0 (pH 9.1). On the basis of the stability constants reported by Corrie et al. and Bizri et al.,[14,16] solution B ($C_{Pb^{II}}$ = 10 mM) would contain a mixture of $[Pb(Cys)(HCys)]^-$ and $[Pb(Cys)_2]^{2-}$ complexes (Figure S-1b

DOI: 10.1021/ic5025668
Inorg. Chem. 2015, 54, 2160–2170

in the SI). The peak maximum λ_{max} = 300 nm in the UV−vis spectrum of solution B is slightly red-shifted relative to that of solution A (mole ratio H_2Cys/Pb^{II} = 2.1; λ_{max} = 298 nm; see Figure S-4a in the SI). The recorded λ_{max} is 310 nm for a PbS_2N_2 complex, where the Pb^{II} ion is surrounded with two histidine and two cysteine residues from synthetic peptide CP-CCHH,[52] and 295 nm for a solution with Pb^{II}/DMSA (DMSA = S,O-chelating agent succimer) in mole ratio 1:100 ($C_{Pb^{II}}$ = 0.02 mM; C_{DMSA} = 2 mM; pH 7.4).[53] Thus, the red shift of λ_{max} to 300 nm for lead(II) cysteine solution B probably is due to an increase in the amount of the $[Pb(S,N\text{-}Cys)_2]^{2-}$ complex in this solution, although the UV−vis spectra cannot exclude PbS_2O_2-coordinated species. Moreover, solution B has higher absorption at $\lambda \sim 330$ nm than solution A (Figure 2), which can be attributed to the presence of a minor amount of a trithiolate lead(II) complex (see below).

This indication of a decrease in the amount of lead(II) species with PbS_2NO coordination is further supported upon comparison of the ^{13}C NMR chemical shifts of the carboxylate group for solutions A (180.9 ppm) and B (177.3 ppm), relative to that of free cysteine at similar pH (175.9 ppm); see Figure 3. The signal is considerably less deshielded for solution B [$\Delta\delta(^{13}C)$ = 1.4 ppm] than for solution A (5.0 ppm; see Table S-2 in the SI), which is probably due to less involvement of the cysteine carboxylate group $-COO^-$ in binding to the Pb^{II} ions in solution B. For the corresponding lead(II) penicillamine solutions, with H_2Pen/Pb^{II} = 2.0−3.0 and $C_{Pb^{II}}$ = 10 mM, the differences $\Delta\delta(^{13}C)$ relative to $\delta_C(COO^-)$ of free penicillamine (pH 9.6), were adequately consistent (6.0−6.5 ppm), signifying that the coordination mode of penicillamine did not change.[26]

The ^{207}Pb NMR signal for solution B appears as a rather broad peak at 2112 ppm, deshielded ∼100 ppm relative to solution A. This chemical shift is close to the isotropic chemical shift of the crystalline $Pb(S,N\text{-aet})_2$ complex (δ_{iso} = 2105 ppm; Figure 5) and further deshielded relative to $\delta(^{207}Pb)$ = 1833 ppm of the $[Pb(S,N,O\text{-Pen})(S\text{-HPen})]^-$ complex with PbS_2NO coordination in a similar lead(II) penicillamine solution (pH 9.6).[26] Therefore, solution B contains more of the $[Pb(Cys)_2]^{2-}$ (PbS_2N_2) and less of the $[Pb(Cys)(HCys)]^-$ (PbS_2NO) (and $[Pb(Cys)(OH)]^-$) complexes than solution A. Nevertheless, the EXAFS spectra and corresponding Fourier transforms for solutions A and B overlap (Figure S-8 in the SI) because N and O atoms, adjacent in the periodic table, cannot be distinguished by this technique. Also, the presence of a minor amount of a trithiolate lead(II) complex could contribute to the deshielding of the ^{207}Pb NMR signal for solution B (see below).

For the more concentrated lead(II) cysteine solution B* ($C_{Pb^{II}}$ = 100 mM) with the same mole ratio H_2Cys/Pb^{II} = 3.0, the ^{207}Pb NMR signal appeared at 2219 ppm (Figure 4). Because the shielding increases in the order S < N < O,[27] we initially assumed that this deshielding of ∼200 ppm relative to solution A* would be due to the formation of some amount of a $[Pb(S\text{-HCys})_3]^-$ complex at the higher free cysteinate concentration in B* because the observed ^{207}Pb NMR chemical shift for the $Pb(S\text{-GSH})_3$ complex with PbS_3 coordination is 2793 ppm.[33] However, the fitting of linear combinations of EXAFS oscillations to the EXAFS spectra (Figure S-11b in the SI) showed that solution B* contains ∼23% of a lead(II) complex with PbS_3N coordination (20% in solution B; error limit ±10−15% in Table 3). Although the EXAFS fitting cannot differentiate between O and N scattering, their different ^{207}Pb NMR shielding abilities (N < O) imply that the additional deshielding of the ^{207}Pb NMR signals for solutions B and B* probably is due to the partial formation of a $[Pb(S,N\text{-Cys})(S\text{-HCys})_2]^{2-}$ complex with PbS_3N coordination and an increased amount of the $[Pb(S,N\text{-Cys})_2]^{2-}$ (PbS_2N_2) complex relative to solutions A and A*. The further deshielding of ∼100 ppm for solution B* relative to solution B would be due to a higher amount of $[Pb(S,N\text{-Cys})_2]^{2-}$ and $[Pb(S,N\text{-Cys})(S\text{-HCys})_2]^{2-}$ complexes in B*, which has a higher free cysteine concentration than solution B.

Because the formation of a trithiolate complex was not reported by either Bizri et al. or Crea et al., the fraction diagrams in Figures S-1b and S-2b in the SI for H_2Cys/Pb^{II} mole ratios ≥3.0 do not fully reflect the chemical composition of solutions B−F and B*−F*. Conversely, the formation constant of $Pb(Cys)_3^{4-}$ proposed by Corrie et al. ($\log\beta$ = 22.47 at 25 °C; I = 3.00 M $NaClO_4$)[13] clearly overestimates the total amount of trithiolate species in those solutions.

Least-squares curve fitting of the EXAFS spectra for solutions B and B*, using a model with Pb−(N/O) and Pb−S scattering paths, resulted in the average distances 2.43 ± 0.04 and 2.64 ± 0.04 Å, respectively (Table 4). The refined coordination number for the Pb−S path was slightly higher (2.3) for solution B* relative to that of solution A* (2.0), another indication of a minor amount of trithiolate complexes in the former solution. This is also evident from the difference in amplitude upon comparison of the EXAFS oscillations and the corresponding Fourier transforms for solutions A* and B* (Figure S-8 in the SI). It can be concluded that in solution B* the $[Pb(S,N\text{-Cys})_2]^{2-}$ complex dominates, with minor amounts of $[Pb(S,N,O\text{-Cys})(S\text{-HCys})]^-$ and $[Pb(S,N\text{-Cys})(S\text{-HCys})_2]^{2-}$ species being present.

Solutions with $H_2Cys/Pb^{II} \geq 4.0$ (pH 9.1). For solutions C and D ($C_{Pb^{II}}$ = 10 mM; H_2Cys/Pb^{II} mole ratios 4.0−5.0), the ^{13}C NMR resonance for the carboxylate group (C1) shows a slight downfield shift ($\Delta\delta_C$) = 1.0−1.4 ppm relative to free cysteinate (Table S-2 in the SI). This resonance, which is an average signal for both free ligand and Pb^{II}-bound cysteinate, indicates that there is still some $[Pb(S,N,O\text{-Cys})(S\text{-HCys})]^-$ present in these solutions. In the UV−vis spectra of solutions C−G ($C_{Pb^{II}}$ = 10 mM; H_2Cys/Pb^{II} mole ratios 4.0−15.0), the intensity of the peak at ∼300 ppm gradually decreases as the free ligand concentration increases. Meanwhile, a growing shoulder appears at ∼330 nm in the spectra of solutions E−G, which is somewhat blue-shifted relative to λ_{max} = 335 nm observed for $Pb(S\text{-GSH})_3$ in the spectra of the corresponding lead(II) glutathione solutions (Figure 2).[33] The difference between the UV−vis spectra of solutions G (pH 9.15) and G′ (pH 8.95) with high ligand excess (mole ratio H_2Cys/Pb^{II} = 15, which means ∼0.12 M free cysteinate) shows a clear maximum at 335 nm similar to the λ_{max} value of $Pb(S\text{-GSH})_3$; see Figure 2 (left), indicating an increased amount of the $[Pb(S\text{-HCys})_3]^-$ complex in solution G′. This is consistent with an increase in the protonation of the amine group in the free cysteine ligands, thus promoting PbS_3 coordination as the pH is lowered by 0.2 units. The crossing points of the UV−vis spectra of solutions F and G with H_2Cys/Pb^{II} mole ratios 10.0 and 15.0, respectively, with that of solution A are very close at 312.2 nm (Figure S-4b in the SI), which probably implies that the less stable dithiolate $[Pb(S,N,O\text{-Cys})(S\text{-HCys})]^-$ has been completely converted to a trithiolate lead(II) species. Interconversion then occurs between the dithiolate $[Pb(S,N\text{-Cys})_2]^{2-}$ and the trithiolate $[Pb(S,N\text{-Cys})(S\text{-HCys})_2]^{2-}$ complexes, probably in equilibrium with a minor amount of $[Pb(S\text{-HCys})_3]^-$.

DOI: 10.1021/ic5025668
Inorg. Chem. 2015, 54, 2160−2170

Scheme 1. Proposed Structures for the Major Lead(II) Cysteine Complexes Formed in an Alkaline Aqueous Solution (pH 9.1−10.4): Dithiolates Na[Pb(Cys)(HCys)] and Na_2[Pb(Cys)$_2$] and Trithiolate Na_2[Pb(Cys)(HCys)$_2$] with Proposed λ_{max} (UV−Vis) and $\delta(^{207}Pb)$ Chemical Shifts Based on the Data from [Pb(Pen)(HPen)]$^-$ (PbS_2NO) and [Pb(aet)$_2$] (PbS_2N_2) Complexes

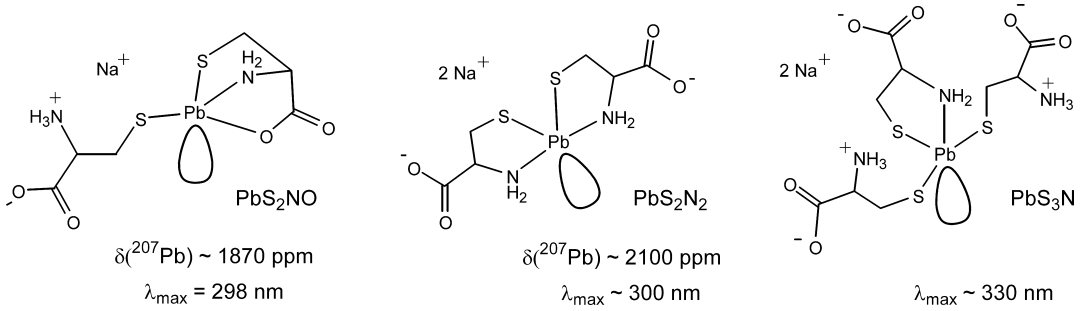

The ESI-MS spectrum of solution F with $C_{Pb^{II}}$ = 10 and 100 mM cysteine showed a mass peak at 635.97 amu for the $[Na_3Pb(Cys)(HCys)_2]^+$ ion (Figure 1 and Table 2), an experimental evidence for the presence of a [Pb(*S*,*N*-Cys)(*S*-HCys)$_2$]$^{2-}$ complex in this solution. However, no mass peak corresponding to the [Pb(*S*-HCys)$_3$]$^-$ ion could be identified.

The ^{207}Pb NMR resonance for solutions C−G shifts downfield from $\delta(^{207}Pb)$ = 2211 to 2387 ppm. For the concentrated solutions C*−F* ($C_{Pb^{II}}$ = 100 mM) with a higher concentration of free cysteinate, the ^{207}Pb NMR peaks appear further downfield (2316−2507 ppm; Figure 4). A linear combination fitting of the EXAFS spectra (Figure S-11b in the SI) showed that the amount of the [Pb(*S*,*N*-Cys)(*S*-HCys)$_2$]$^{2-}$ complex gradually increases in solutions C*−F*, causing a downfield shift of their ^{207}Pb NMR signals (Table 3). This is also evident from the increase in amplitude of the EXAFS oscillation and its corresponding Fourier transform for solution F* (H_2Cys/Pb^{II} = 10.0), compared with those of solutions A* and B* (H_2Cys/Pb^{II} = 2.1−3.0); see Figure S-8 in the SI. According to the linear combination fitting of the EXAFS spectra for lead(II) cysteine solutions E* and F* (with overlapping EXAFS spectra; see Figure S-8 in the SI), they contain ∼50% dithiolate (PbS_2NO + PbS_2N_2) and ∼50% trithiolate (PbS_3N + PbS_3) species (±10%; see Table 3 and Figure S-11b−e and Table S-3 in the SI). Assuming that the successive movement of the crossing point of the UV−vis spectra corresponds to a gradual conversion primarily of the PbS_2NO-coordinated dithiolate as the amount of trithiolate complexes increases (see above), it is very likely that solutions D*−F* (H_2Cys/Pb^{II} = 5.0−10.0) with free cysteinate concentrations of ≥0.2 M have little to no PbS_2NO complex present. Even with this assumption, it is not possible to propose an exact value for the ^{207}Pb NMR chemical shift of a [Pb(*S*,*N*-Cys)(*S*-HCys)$_2$]$^{2-}$ (PbS_3N) complex based on the observed chemical shifts for solutions D*−F*, considering $\delta_{Pb}(PbS_2N_2)$ = 2105 ppm and $\delta_{Pb}(PbS_3)$ = 2793 ppm. The calculated $\delta_{Pb}(PbS_3N)$ value fluctuates over wide ranges (from 2767 to 2925 ppm and from 2488 to 2771 ppm, respectively) based on the relative percentages of PbS_2N_2 and PbS_3N (and PbS_3) species in solutions D*−F* from Tables 3 and S-3 in the SI.

In the model for EXAFS least-squares curve fitting for solution F*, a 50:50% mixture of complexes with PbS_2N(N/O) and PbS_3N coordination was initially assumed with fixed path frequencies (*N*), 1.5 for Pb−(N/O) and 2.5 for Pb−S (Table S-4, model V, in the SI). However, a slightly better residual was obtained when the frequency of the Pb−S path was refined to 2.9, indicating that the amount of the PbS_3N complex could be even somewhat higher (>50%) in this solution and then also in solution E* (Table 4).

While the average Pb−(N/O) distance (2.43 ± 0.04 Å) obtained for solution F* is consistent with those obtained for solutions A* and B* (Table 4), the mean Pb−S bond distance became somewhat longer (2.66 ± 0.04 Å). Such an $(Pb-S)_{ave}$ elongation is expected because the corresponding distances that gave the best results when the EXAFS oscillation was simulated for PbS_3N coordination in the EXAFS linear combination fitting procedure were Pb−N 2.40 Å and Pb−S 2.68 Å (see the Results section). A survey in the Cambridge crystal structure database (CSD; Nov 2013)[49] shows only a few crystalline compounds with PbS_3N coordination (Table S-6 in the SI), all of which are multinuclear complexes with bridging thiolate groups. Only in one case do both amine and thiolate groups surround the Pb^{II} ion (CSD: PAQVOT), with the bond distances Pb−N 2.411 Å and Pb−S 2.704, 2.892, and 3.086 Å (the latter two are bridging).[45]

In summary, the lead(II) cysteine solutions in the current study show ^{207}Pb NMR chemical shifts (∼2000−2500 ppm) in the range between those of the corresponding lead(II) penicillamine and Pb(GSH)$_3$ solutions with PbS_2NO (∼1870 ppm) and PbS_3 (2793 ppm) coordination geometries, respectively, and are close to the isotropic chemical shift of solid Pb(*S*,*N*-aet)$_2$ (2105 ppm) with PbS_2N_2 coordination. A linear combination fitting of the EXAFS spectra confirms that complexes with PbS_2N(N/O) and PbS_3N coordination give major contributions to the experimental EXAFS spectra obtained for these lead(II) cysteine solutions. Therefore, we propose that a mixture of lead(II) species with PbS_2N(N/O) and PbS_3N coordination dominates in the alkaline lead(II) cysteine solutions (pH 9.1). The dithiolate [Pb(*S*,*N*-Cys)$_2$]$^{2-}$ and [Pb(*S*,*N*,*O*-Cys)(*S*-HCys)]$^-$ complexes, both with PbS_2N-(N/O) coordination, display their maximum UV−vis absorption at λ_{max} ∼ 298−300 nm and average Pb−S and Pb−N distances at 2.64 ± 0.04 and 2.42 ± 0.04 Å, respectively. The absorption of the trithiolate [Pb(*S*,*N*-Cys)(*S*-HCys)$_2$]$^{2-}$ complex with PbS_3N coordination appears as a shoulder at about λ ∼ 330 nm, and its average Pb−S and Pb−N distances are estimated to 2.68 ± 0.04 Å (σ^2 = 0.0065 ± 0.002 Å^2) and 2.40 ± 0.04 Å (σ^2 = 0.008 ± 0.002 Å^2), respectively. However, a specific ^{207}Pb NMR chemical shift could not be assigned to this complex. When the pH is lowered by 0.2 units to 8.95 in solution G′ with a high free cysteinate concentration (∼0.12 M), a clear contribution to the UV−vis absorption at λ ∼ 330 nm emerges, identified through the spectral difference at λ_{max} = 335 nm, which we ascribe to a minor amount of a [Pb(*S*-HCys)$_3$]$^-$ complex with PbS_3 coordination, although the exact

DOI: 10.1021/ic5025668
Inorg. Chem. 2015, 54, 2160−2170

amount is difficult to obtain for the solutions and at the pH values used in the current study.

Scheme 1 presents our proposed structures for the major lead(II) cysteine complexes in an alkaline solution (pH ~9.1−10.4). The positions of the stereochemically active, partially occupied antibonding molecular orbitals in PbS_2N_2 and PbS_3N coordination sites follow the two different models proposed for four-coordinated lead(II) complexes in an earlier theoretical study.[54]

CONCLUSION

Lead(II) precipitates as a 1:1 PbCys solid compound from mildly acidic and neutral solutions of the amino acid cysteine.[18,50,51] The precipitate dissolves in alkaline media; the higher the free cysteinate concentration, the lower the pH at which the solid dissolves. The current study shows that a mixture of the dithiolate $[Pb(S,N,O\text{-Cys})(S\text{-HCys})]^-$ and $[Pb(S,N\text{-Cys})_2]^{2-}$ complexes dominates at the H_2Cys/Pb^{II} mole ratio 2.1 (pH 10.4). Both complexes are consistent with the $Pb(HCys)(Cys)^-$ and $Pb(Cys)_2^{2-}$ species, respectively, reported for alkaline solutions by Bizri et al.,[16] while the stability constants recently reported by Crea et al. for very dilute solutions only describe the $[Pb(S,N\text{-Cys})_2]^{2-}$ complex (Figure S-2b in the SI).[20]

Increasing ligand excess in our series of solutions promotes the further formation of $[Pb(S,N\text{-Cys})_2]^{2-}$ (major) as well as the trithiolate $[Pb(S,N\text{-Cys})(S\text{-HCys})_2]^{2-}$ complex. Finally, when the free cysteinate concentration exceeds 0.7 M, the trithiolate species form about 50% of the solution composition (pH 9.1). Also, minor amounts of the dithiolate $[Pb(S,N,O\text{-Cys})(S\text{-HCys})]^-$ and trithiolate $[Pb(S\text{-HCys})_3]^-$ complexes are in equilibrium with the above two major species.

The current study shows that in alkaline lead(II) cysteine solutions with mole ratios $H_2Cys/Pb^{II} > 2.1$, pH 9.1, both the dithiolate $[Pb(S,N\text{-Cys})_2]^{2-}$ and trithiolate $[Pb(S,N\text{-Cys})(S\text{-HCys})_2]^{2-}$ complexes with at least one cysteinate ligand in bidentate coordination mode persist, in contrast to the closely related chelating agent penicillamine that binds strongly to the Pb^{II} ion in a tridentate mode in the $[Pb(S,N,O\text{-Pen})(S\text{-H}_n\text{Pen})]^{2-n}$ ($n = 0-1$) complex with high stability in alkaline solutions (pH 9.6). Furthermore, while a high excess of free cysteinate is required for the formation of trithiolate lead(II) complexes, the $Pb(S\text{-GSH})_3$ complex dominates at much lower free glutathione concentration already at pH 8.5[33] because cysteine, but not glutathione, is able to form a five-membered S,N-chelate ring, stabilizing the $[Pb(S,N\text{-Cys})_2]^{2-}$ and $[Pb(S,N\text{-Cys})(S\text{-HCys})_2]^{2-}$ complexes. Even though the pH dependence of the UV−vis spectra shows that a minor amount of the $[Pb(S\text{-HCys})_3]^-$ complex with monodentate PbS_3 coordination forms, it is in a minor amount.

Our proposed structures in Scheme 1 for bis(cysteinate)-lead(II) complexes with *hemidirected*[55] PbS_2NO and PbS_2N_2 coordination in solution differ from that recently proposed for a $[Pb(S,N,O\text{-Cys})_2]^{2-}$ complex, which was based on a single XAS study of a lead(II) cysteine solution ($C_{Pb^{II}} = 40$ mM; pH 7.7),[56] assuming Pb^{II} to be bound to two tridentate cysteinate ligands with $PbS_2N_2O_2$ coordination. The ^{207}Pb NMR resonance for such a six-coordinated lead(II) species would be expected further upfield than our observed values, such as, e.g., for the $(Ph_4As)[Pb(SOCPh)_3]$ complex with PbS_3O_3 coordination ($\delta_{Pb} = 1422-1463$ ppm).[57] The resemblance of our reported isotropic chemical shift ($\delta_{iso} = 2105$ ppm) for the crystalline bis(2-aminoethanethiolato)lead(II) complex, $Pb(S,N\text{-aet})_2$, to the ^{207}Pb NMR chemical shifts observed for our alkaline lead(II) cysteine solutions further supports the proposed four-coordinated structure for the $[Pb(S,N\text{-Cys})_2]^{2-}$ complex.

The results obtained in the current study indicate that the differences in the structures of the PbS nanoparticles obtained from lead(II) cysteine solutions with different ligand-to-metal mole ratios, concentrations, and pH values probably are connected to changes in the coordination. Moreover, the results provide "spectroscopic fingerprints" for different coordination environments in lead(II) thiolate complexes, which are of general value to assess structural models for lead(II) binding to proteins and enzymes.

ASSOCIATED CONTENT

Supporting Information

Fraction diagrams for lead(II) cysteine complexes calculated using the *MEDUSA* program, ESI-MS spectrum of solution F (negative-ion mode) and assignment of the mass ions, a comparison between the UV−vis spectra of lead(II) solutions containing H_2Cys/Pb^{II} mole ratios 2.1−3.0, and H_2Pen/Pb^{II} mole ratio 3.0, ^{207}Pb NMR spectrum of an aqueous solution of $Pb(aet)_2$ + Haet, a comparison between the reconstructed static ^{207}Pb NMR powder pattern and MAS ^{207}Pb NMR spectra of $Pb(aet)_2$, a comparison between Pb L_{III}-edge XANES spectra for solutions (A, E) and (A*, F*), and EXAFS spectra for the two sets ($C_{Pb^{II}} = 10$ and 100 mM), together with their least-squares curve-fitting results using different models, PCA analysis and linear combination fitting for the EXAFS spectra of solutions A*−F* and A−E, and survey of the crystal structure database for PbS_3N complexes. This material is available free of charge via the Internet at http://pubs.acs.org.

AUTHOR INFORMATION

Corresponding Author

*E-mail: faridehj@ucalgary.ca.

Notes

The authors declare no competing financial interest.

ACKNOWLEDGMENTS

We are grateful to Dr. Michelle Forgeron, Qiao Wu, Jian Jun (Johnson) Li, and Dorothy Fox at the instrumentation facility at the Department of Chemistry, University of Calgary, for their assistance with NMR measurements and to Wade White for measuring the ESI-MS spectra. Special thanks go to Dr. Patrick Frank (Stanford University) for helpful discussions. The solid-state ^{207}Pb NMR spectrum for crystalline $Pb(aet)_2$ was measured at the Department of Chemistry, University of Ottawa. XAS measurements were carried out at the SSRL (Proposals 2848 and 3637). Use of the SSRL, SLAC National Accelerator Laboratory, is supported by the U.S. Department of Energy (DOE), Office of Science, Office of Basic Energy Sciences, under Contract DE-AC02-76SF00515. The SSRL Structural Molecular Biology Program is supported by the DOE Office of Biological and Environmental Research and by the National Institutes of Health (NIH), National Institute of General Medical Sciences (NIGMS; including P41GM103393). The contents of this publication are solely the responsibility of the authors and do not necessarily represent the official views of NIGMS or NIH. We acknowledge the National Science and Engineering Research Council of Canada (NSERC), the Canadian Foundation for Innovation (CFI), the Province of Alberta (Department of Innovation and Science), and the

DOI: 10.1021/ic5025668
Inorg. Chem. 2015, 54, 2160−2170

University of Calgary (Faculty of Science) for their financial support.

DEDICATION

Dedicated to Professor Magnus Sandström on the occasion of his 70th birthday.

REFERENCES

(1) Cobbett, C.; Goldsbrough, P. *Annu. Rev. Plant Biol.* **2002**, *53*, 159−182.
(2) Carpene, E.; Andreani, G.; Isani, G. *J. Trace Elem. Med. Biol.* **2007**, *21 S1*, 35−39.
(3) Fischer, K. *Water Air Soil Poll.* **2002**, *137*, 267−286.
(4) Vadas, T. M.; Ahner, B. A. *J. Environ. Qual.* **2009**, *38*, 2245−2252.
(5) Wang, S.; Mulligan, C. N. *Environ. Geochem. Health* **2013**, *35*, 111−118.
(6) Vandenbossche, M.; Casetta, M.; Jimenez, M.; Bellayer, S.; Traisnel, M. *J. Environ. Manage.* **2014**, *132*, 107−112.
(7) Li, L.; Wu, J.; Zhao, M.; Wang, Y.; Zhang, H.; Zhang, X.; Gui, L.; Liu, J.; Mair, N.; Peng, S. *Chem. Res. Toxicol.* **2012**, *25*, 1948−1954.
(8) Xiong, S.; Xi, B.; Xu, D.; Wang, C.; Feng, X.; Zhou, H.; Qian, Y. *J. Phys. Chem. C* **2007**, *111*, 16761−16767.
(9) Zuo, F.; Yan, S.; Zhang, B.; Zhao, Y.; Xie, Y. *J. Phys. Chem. C* **2008**, *112*, 2831−2835.
(10) Thongtem, T.; Kaowphong, S.; Thongtem, S. *Ceram. Int.* **2008**, *34*, 1691−1695.
(11) Shen, X. F.; Yan, X. P. *J. Mater. Chem.* **2008**, *18*, 4631−4635.
(12) Shen, X. F.; Yan, X. P. *Angew. Chem., Int. Ed.* **2007**, *46*, 7659−7663.
(13) Corrie, A. M.; Touche, M. L. D.; Williams, D. R. *J. Chem. Soc., Dalton Trans.* **1973**, 2561−2565.
(14) Corrie, A. M.; Walker, M. D.; Williams, D. R. *J. Chem. Soc., Dalton Trans.* **1976**, 1012−1015.
(15) Corrie, A. M.; Williams, D. R. *J. Chem. Soc., Dalton Trans.* **1976**, 1068−1072.
(16) Bizri, Y.; Cromer-Morin, M.; Schaeff, J.-P. *J. Chem. Res., Synop.* **1982**, 192−193.
(17) Li, N. C.; Manning, R. A. *J. Am. Chem. Soc.* **1955**, *77*, 5225−5228.
(18) Shindo, H.; Brown, T. L. *J. Am. Chem. Soc.* **1965**, *87*, 1904−1909.
(19) Pardo, R.; Barrado, E.; Gutiérrez, H.; Sánchez Batanero, P. *Quim. Anal. (Barcelona)* **1991**, *10*, 103−113.
(20) Crea, F.; Falcone, G.; Foti, C.; Giuffre, O.; Materazzi, S. *New J. Chem.* **2014**, *38*, 3973−3983.
(21) Kane-Maguire, L. A. P.; Riley, P. J. *J. Coord. Chem.* **1993**, *28*, 105−120.
(22) Glasoe, P. K.; Long, F. A. *J. Phys. Chem.* **1960**, *64*, 188−190.
(23) Hershenson, H. M.; Smith, M. E.; Hume, D. N. *J. Am. Chem. Soc.* **1953**, *75*, 507−511.
(24) Wrathall, D. P.; Izatt, R. M.; Christensen, J. J. *J. Am. Chem. Soc.* **1964**, *86*, 4779−4783.
(25) Fleischer, H.; Schollmeyer, D. *Inorg. Chem.* **2004**, *43*, 5529−5536.
(26) Sisombath, N.; Jalilehvand, F.; Schell, A. C.; Wu, Q. *Inorg. Chem.* **2014**, *53*, 12459−12468.
(27) Wrackmeyer, B.; Horchler, K.; Webb, G. A. ^{207}Pb-NMR Parameters. In *Annual Report on NMR Spectroscopy*; Webb, G. A., Ed.; Academic Press: San Diego, CA, 1990; Vol. *22*, pp 249−306.
(28) van Gorkom, L. C. M.; Hook, J. M.; Logan, M. B.; Hanna, J. V.; Wasylishen, R. E. *Magn. Reson. Chem.* **1995**, *33*, 791−795.
(29) Willans, M. J.; Demko, B. A.; Wasylishen, R. E. *Phys. Chem. Chem. Phys.* **2006**, *8*, 2733−2743.
(30) Schell, A.; Parvez, M.; Jalilehvand, F. *Acta Crystallogr., Sect. E* **2012**, *E68*, m489−m490.
(31) Zabinsky, S. I.; Rehr, J. J.; Ankudinov, A.; Albers, R. C.; Eller, M. J. *Phys. Rev. B* **1995**, *52*, 2995−3009.
(32) Ankudinov, A. L.; Rehr, J. J. *Phys. Rev. B* **1997**, *56*, R1712−R1716.
(33) Mah, V.; Jalilehvand, F. *Inorg. Chem.* **2012**, *51*, 6285−6298.
(34) George, G. N.; Geroge, S. J.; Pickering, I. J. *EXAFSPAK*; SSRL: Menlo Park, CA, 2001.
(35) *CRC Handbook of Chemistry and Physics*, 80th ed.; CRC Press: Boca Raton, FL, 1999.
(36) Burford, N.; Eelman, M. D.; LeBlanc, W. G. *Can. J. Chem.* **2004**, *82*, 1254−1259.
(37) Magyar, J.; Weng, T.-C.; Stern, C.; Dye, D.; Payne, J.; Bridgewater, B.; Mijovilovich, A.; Parkin, G.; Zaleski, J.; Penner-Hahn, J.; Godwin, H. *J. Am. Chem. Soc.* **2005**, *127*, 9495−9505.
(38) Wang, Y.; Hemmingsen, L.; Giedroc, D. *Biochemistry* **2005**, *44*, 8976−8988.
(39) Ghering, A.; Miller Jenkins, L.; Schenck, B.; Deo, S.; Mayer, A.; Pikaart, M.; Omichinski, J.; Godwin, H. *J. Am. Chem. Soc.* **2005**, *127*, 3751−3759.
(40) Vogler, A.; Nikol, H. *Pure Appl. Chem.* **1992**, *64*, 1311−1317.
(41) Harrison, P. G.; Healy, M. A.; Steel, A. T. *J. Chem. Soc., Dalton Trans.* **1983**, 1845−1848.
(42) Dmitrenko, O.; Bai, S.; Beckmann, P.; Bramer, S.; Vega, A.; Dybowski, C. *J. Phys. Chem. A* **2008**, *112*, 3046−3052.
(43) Van Bramer, S. E.; Glatfelter, A.; Bai, S.; Dybowski, C.; Neue, G.; Perry, D. L. *Magn. Reson. Chem.* **2006**, *44*, 357−365.
(44) Briand, G.; Smith, A.; Schatte, G.; Rossini, A.; Schurko, R. *Inorg. Chem.* **2007**, *46*, 8625−8637.
(45) Bharara, M. S.; Kim, C. H.; Parkin, S.; Atwood, D. A. *Polyhedron* **2005**, *24*, 865−871.
(46) Li, Y.; Martell, A. E. *Inorg. Chim. Acta* **1995**, *231*, 159−165.
(47) Sisombath, N.; Jalilehvand, F. Manuscript in preparation.
(48) Ressler, T. *J. Synchrotron Radiat.* **1998**, *5*, 118−122.
(49) Allen, F. H. *Acta Crystallogr., Sect. B* **2002**, *B58*, 380−388.
(50) Klement, R. *Ber. Dtsch. Chem. Ges. A/B* **1933**, *66*, 1312−1315.
(51) Made Gowda, N. M.; Mahadevappa, D. S. *J. Ind. Chem. Soc.* **1976**, *LIII*, 705−709.
(52) Payne, J.; Horst, M.; Godwin, H. *J. Am. Chem. Soc.* **1999**, *121*, 6850−6855.
(53) Harris, W. R.; Chen, Y.; Stenback, J.; Shah, B. Stability Constants for Dimercaptosuccinic Acid with Bismuth(III), Zinc(II), and Lead(II). *Journal of Coordination Chemistry*; Taylor & Francis: Oxford, U.K., 1991; Vol. *23*, pp 173−186.
(54) Jarzęcki, A. A. *Inorg. Chem.* **2007**, *46*, 7509−7521.
(55) Shimoni-Livny, L.; Glusker, J. P.; Bock, C. W. *Inorg. Chem.* **1998**, *37*, 1853−1867.
(56) Swarbrick, J. C.; Skyllberg, U.; Karlsson, T. r.; Glatzel, P. *Inorg. Chem.* **2009**, *48*, 10748−10756.
(57) Burnett, T. R.; Dean, P. A. W.; Vittal, J. J. *Can. J. Chem.* **1994**, *72*, 1127−1136.

DOI: 10.1021/ic5025668
Inorg. Chem. 2015, 54, 2160−2170